5th International Conference on Experimental Fluid Mechanics ICEFM 2018 Munich
Munich, Germany, July 2-4, 2018

Isothermal PIV Measurement of Planar Film Injection with Regard to Reactive Film Cooling

R. Dalshad*, **M. Straußwald, T. Sander, M. Pfitzner**

Universität der Bundeswehr München, Department of Aerospace Engineering, Munich, Germany

* rahand.dalshad@unibw.de

Abstract

2D PIV measurements are carried out to investigate a planar film cooling geometry and the flow field for isothermal conditions. Main focus is the characterization of the film layer and the interaction zone based on the coolant-to-main stream velocity ratio *VR* from 1.5 to 3.7. Air and CO_2 are applied as coolants to represent different density ratios. The study shows that averaged flow fields from a measurement of 4 s is in good agreement with results from 16 s. For the wall parallel injection, the VR proves to be the appropriate parameter for comparison. The thickening of the film with increasing VR is observed and the distance of the interaction zone is determined based on a velocity deviation of 5 % from the average main flow velocity. The thickness of the film is less than 4 mm in the region of interest. The influence of vertical reinforcements on the cooling film inlet is visible for a considerable distance downstream. The findings are of importance for a future reactive film cooling experiment with a similar setup but Hydrogen or Methane as coolant.

1 Introduction

The high demand of thrust of today's aircraft engines requires thermal operating conditions far beyond the melting point of any applicable material. Therefore, active cooling is necessary to protect components that are subject to high thermal strain. An effective and widely used cooling technique for combustion chamber and turbine blades is film cooling where relatively cold gas is injected as a protective layer to isolate the wall from the hot gas. However, the isolating effect of the cooling gas decreases downstream of the injection because of mixing with the main flow. Furthermore, due to fuel-rich operation of the combustor the hot gas contains residual unburnt fuel and its temperatures are above the auto-ignition point of the fuel. In combination with oxygen containing cooling air this can lead to chemical reactions and heat release within the cooling film. Those secondary combustions cause increased thermal loads on the surface.

Few studies are available investigating secondary combustion in detail. Evans (2008) was one of the first visualizing the secondary reactions downstream of angled cooling air injection. He determined the augmented heat transfer to the surface using thermocouples. The results showed that both, cooling geometry and blowing ratio are the key elements affecting the position of the secondary reactions. Kostka et al. (2011) analyzed the reaction zone and fluid temperature distribution downstream of Evans' angled cooling geometries, using two-color planar laser-induced fluorescence (PLIF). The images show flames anchored to the wall for the slot and for fan shaped cooling holes. Furthermore, the results depict long reaction zones in flow direction for the slot geometry near the wall due to high air mass flow. Also, the temperature reduction within the reaction zone indicated heat transfer to the wall. In contrast, the flames from normal holes (holes oriented normally to the flow direction) are anchored to the hole and the coolant penetrates farther into the main stream generating flames larger by factor of two in the normal direction. Richardson et al. (2014) performed isothermal PIV measurements for angled slot injection to characterize the flow region affected by the cooling film. 50 image pairs were recorded and post-processed. The blowing ratio was varied from 0.5 to 7.0. The data show that even for the highest blowing ratio of 7.0 the zone affected by the coolant is around 5 mm above the wall. The results were consistent with the PLIF measurements of Kostka et al. (2011).

Other setups and film cooling geometries are hardly investigated for reactive conditions. Though, planar injection is often used to apply the starter film at the upstream end of the combustion chamber. It is preferred over angled injection since the cooling effectiveness increases with smaller angle of injection, reported by Goldstein (1971). Commonly used parameters to characterize the behaviour of the coolant film

are density ratio $DS = \rho_c/\rho_m$, velocity ratio $VR = U_c/U_m$, blowing ratio $M = DR \cdot VR$ and momentum ratio $I = DR \cdot (VR)^2$, where ρ indicates the fluid mass density, U the bulk velocity, and the subscripts c and m indicate the cooling stream and main stream, respectively. For a three-dimensional jet penetrating the main stream primarily the momentum is relevant for comparison. The blowing ratio is of interest as correlation parameter for predicting film cooling effectiveness. But in case of flow separation, the momentum ratio can also be of importance, according to Goldstein and Eckert (1974). Johnson et al. (2014) performed further PIV measurements on angled film cooling injection for air and CO_2 to analyse the effect of the density ratio. It was found that for a constant blowing ratio the coolant with the higher density was likely to stay attached to the surface. However, the blowing ratio seems to be insufficient to characterize the flow field individually. Schreivogel et al. (2014) compared VR, M and I of numerically and experimentally investigated angled film cooling geometries. It was found that for constant M the coolant jet penetration increases with decreasing density ratio. But for constant VR the penetration decreases for lower density ratios, consistent to the conclusions of Johnson. Furthermore, the results suggest that the velocity ratio determines the mixing of the streams. One explanation was that the interaction and mixing of the two streams are rather controlled by velocity and diffusion than mass and momentum.
Planar and angled injection has been investigated extensively for non-reactive conditions. The aim of the current study is the investigation of planar film injection for isothermal conditions using air and CO_2 as coolants. The results form the basis for an upcoming reactive film cooling analysis with flammable coolants such as Hydrogene or Methane. The hot main stream will contain residual oxygen allowing secondary reactions. Cooling with fuel is applied in rocket chambers and represents the inverse configuration of Evans. The isothermal study helps to locate the interaction and mixing zone of the two streams.

2 Experimental setup and data acquisition

For the current isothermal investigations, a straightforward design of the burner and the test section were built from aluminum and glass. Inner dimensions of the burner and the test section correspond to the dimensions of the future high-temperature setup. The main flow runs through the burner plenum, goes through a flame-breaker and enters the test section module through a contraction nozzle. Figure 1 shows a sectional view of the test section module. Glass windows (not shown in the figure) form a rectangular duct (50 mm × 53 mm) above the film cooling plate, allowing full optical access to the test section from three sides of the test bench. At $x = 0$, cooling air is injected parallel to the main flow through a slot (42 mm × 2 mm) separated with 1 mm bars generating a set of 10 rectangular holes (3.3 mm × 2 mm). Downstream of the test section a radial blower takes away the exhaust gas.

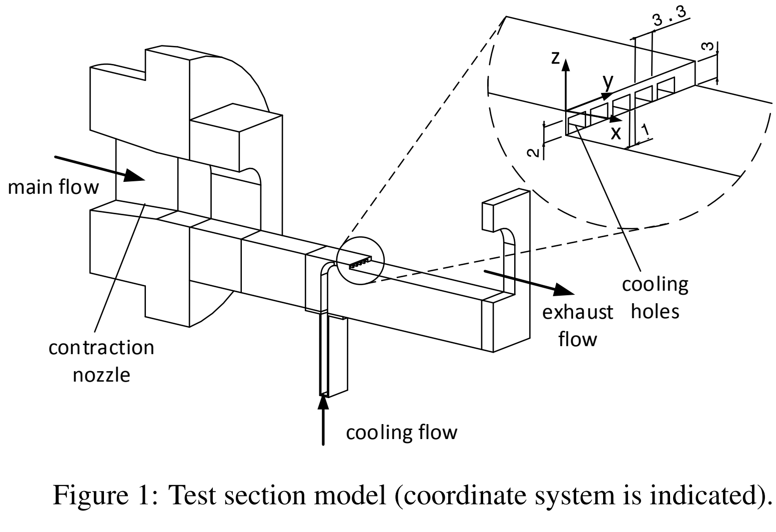

Figure 1: Test section model (coordinate system is indicated).

Main flow and cooling air were controlled with two mass flow meters (Bronkhorst - main flow: F-203AV-1M0-RGD-44-V, cooling air: F-203AV-M50-RGD-44-V) that were operated with Flow DDE software (Bronkhorst). Volume flows of main flow and cooling air were calculated from chosen operating points (velocity ratio and density ratio) and the size of the inlet cross section in the test section module. Main flow was supplied by pressured air. The volume flow was kept constant at 1000 l/min, resulting in a nominal main flow velocity of 6.67 m/s throughout the full set of experiments. Pressured air or CO_2 was used as cooling

gas to realize density ratios of $DR = 1$ and $DR = 1.57$, respectively.
A wide range of velocity ratios was investigated by adapting the volume flow of the cooling film. Furthermore, two positions in y-direction were chosen for measurements downstream of a cooling hole ($y = 2.15$) and downstream of a bar ($y = 0$), called *hole configuration* and *bar configuration*, respectively. Unfortunately, the measured average main flow velocity was 9.12 m/s which is 37 % higher compared to the nominal value. As the temperature was not measured in the test setup, we were not able to find out the cause of the increased velocity and had to keep the nominal values for the density ratio. Nevertheless, we updated the velocity ratios based on the measured main flow velocity. The calculated turbulence intensity of the main flow before the backward facing step is 7 %. A list of all test cases is given in Table 1.
PIV measurements were carried out to characterize the flow conditions for future high-temperature investigations. Main flow and cooling air were individually seeded with aluminum oxide (Al_2O_3) particles. The seeding density could be manually adjusted by increasing the gas flow through the seeders. The experimental setup is shown in Figure 2. A frequency doubled Nd:YAG laser (532 nm, Gemini 200-15, New Wave Research) was operated at 12 Hz double-pulse repetition rate. A $f = -15\ mm$ cylindrical and a $f = 500\ mm$ spherical lens were used to form a laser sheet perpendicular to the test plate. A CMOS high-speed camera (Vision Research, Phantom v710) was used to record the Mie scattered light in the measurement plane.

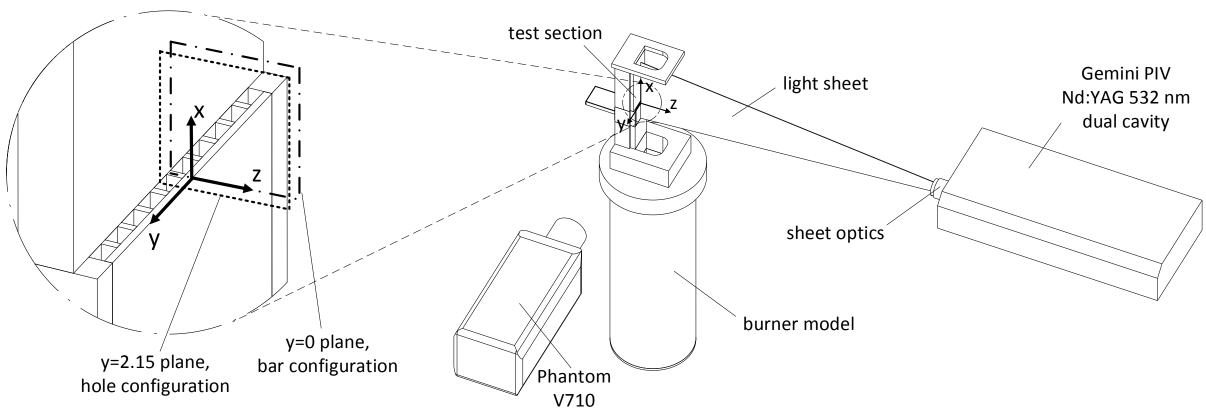

Figure 2: Experimental setup and laser sheet positions.

The resolution was set to 1280 pxl x 800 pxl and the camera was triggered to record double frame images at a repetition rate of 12 Hz. A bandpass filter (BrightLine HC 540-15, AHF Analysetechnik) was used to reduce noise signal on the detector. All relevant parts of the test section module, including the back side of the glass channel, and in the surrounding area were covered with black paint to reduce reflections of the laser light. The raw images were imported into DaVis 8.4 (LaVision) and vector displacement fields were calculated using an adaptive multi-pass cross-correlation algorithm with a final window size of 32 pxl $\times$ 32 pxl and an overlap of 75%. Final post processing was carried out in Matlab 2016b. Velocity fields were calculated from pulse separation (31 µs) and magnification (0.0769 mm/pxl), resulting in a vector spacing of 0.6 mm. The region of interest was defined as $-3.0 \leq x/h \leq 30$ and $-1.5 \leq z/h \leq 6$.

cooling gas	**density ratio DR**	**velocity ratio VR**	**velocity uncertainty***
air	1.0	1.5	0.59
air	1.0	2.2	0.86
air	1.0	2.9	1.03
air	1.0	3.7	1.40
CO_2	1.57	1.5	0.50
CO_2	1.57	2.2	0.76
CO_2	1.57	2.9	1.10
CO_2	1.57	3.7	1.66

Table 1: Film cooling test cases defined by density ratio and velocity ratio.
*Average velocity uncertainty (m/s) in the cooling film.

Pixel displacement uncertainty fields were calculated with a built-in function of DaVis (Wieneke (2015)) and processed similar to the vector displacement fields using pulse separation time and magnification. Unaffected areas in the main flow and the cooling film were chosen to calculate mean velocity uncertainty from the resulting velocity uncertainty fields. The average main flow velocity uncertainty was 0.65 m/s and the maximum velocity uncertainty for the high-velocity cooling film was 1.66 m/s which means a maximum deviation of 6.7 %.

3 Results

Figure 3 shows the average velocity field downstream of the hole configuration for a density ratio of $DR = 1.0$ and a velocity ratio of $VR = 2.2$. The contour plot indicates the absolute velocity field and the arrows indicate its direction. Grey areas illustrate walls and white areas illustrate regions without reasonable data, in particular close to the wall and inside the hole. The coordinate system is normalized with the height of the hole $h = 2\ mm$ and the origin is located at the edge of the backward facing step. It can be observed that the shear layer thickness increases and the velocity reduces along the streamwise coordinate x, but the film stays close to the wall throughout the evaluated domain.

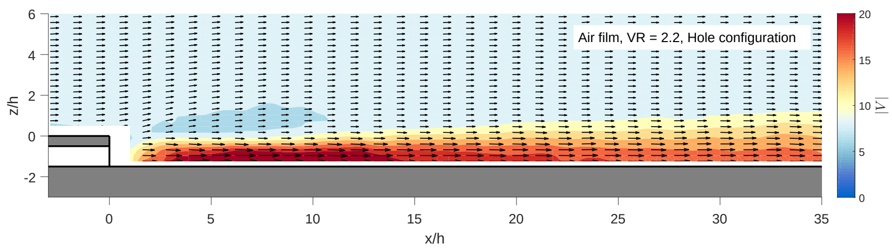

Figure 3: Contour plot air film, $VR = 2.2$.

For easy comparison of the different flow conditions, the boundary layer thickness of the cooling film was calculated for every test case. A deviation of 5 % from the average main flow velocity was defined to be the upper limit of the cooling film. The resulting data points are smoothed with Matlab's polyfit function which is a quadratic polynomial curve function. For the hole configuration, boundary layers are calculated between $2.2 \leq x/h \leq 30$. For the bar configuration, the boundary layer calculation was limited to $5.2 \leq x/h \leq 30$ due to a wake region downstream of the bars.
Figure 4 illustrates the effects of an extended measurement duration. The measurements are carried out for 4 s and 16 s (corresponding to 48 and 192 image pairs), respectively. It can be observed that the boundary layers and the velocity profiles are in good agreement, except for the region close to the cooling hole exit. The 16 s measurement shows a lower velocity near the hole exit compared to the 4 s measurement and compared to regions further downstream. This is physically not plausible, since the film velocity should decrease according to conservation of mass during the thickening process and while interacting with the surrounding main flow. The difference is caused by particle deposition on the glass duct which increases over time and obstructs the camera from recording the particles in the flow. This shows that 48 image pairs are generally enough for averaging the flow field and extended measurements would actually reduce the quality of the result close to the hole exit. Therefore, all other measurements were carried out for 4 s only.

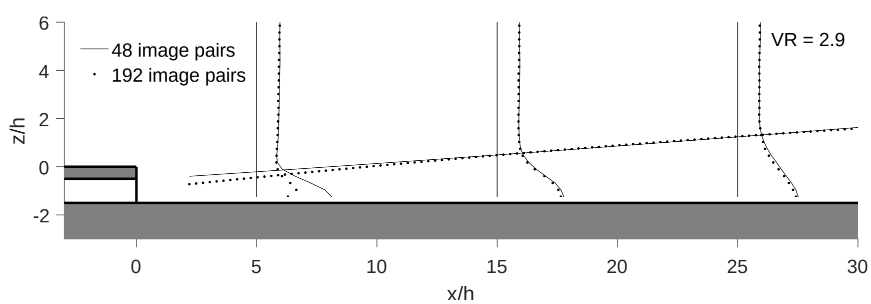

Figure 4: Boundary layer and velocity profiles for air cooling film - 48 image pairs vs 192 image pairs.

To identify density ratio effects, similar measurements of air ($DR = 1$) and CO_2 ($DR = 1.57$) cooling films are evaluated. For comparison of the resulting flow fields Figure 5 illustrates the position of the shear layer and wall normal profiles of the streamwise velocity field at three locations downstream of the coolant injection. The upper image shows the results for constant blowing ratio and the lower image for constant velocity ratio. It can be observed that the shear layer and the velocity profiles are in good agreement for constant velocity ratio whereas there is poor agreement for constant blowing ratio. In literature, the blowing ratio is commonly used to characterize flow conditions for film cooling investigations. The present data, however, indicate that the velocity ratio meets the flow conditions better than the blowing ratio. Therefore, we recommend to use the velocity ratio instead of blowing ratio for future wall parallel film cooling investigations. Furthermore, all following discussions apply for measurements with similar velocity ratio, independent of the density ratio.

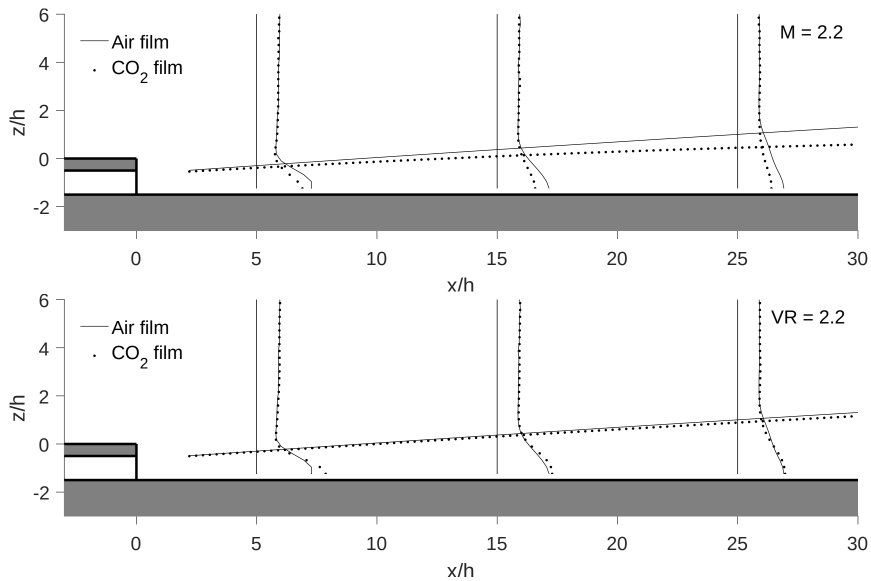

Figure 5: Comparison of blowing ratio (upper part) and velocity ratio (lower part).

Figure 6 depicts the propagation of the boundary layer in streamwise direction and at different velocity ratios. The data are taken from air measurements and hole configuration. It can be observed that the cooling film spreads with increasing distance to the injection point. Furthermore, with increasing velocity ratio the spreading is even stronger. At $x/h = 30$, the distance of the interaction zone from the wall for $VR = 3.7$ is $z/h = 1.77$ or 3.54 mm.

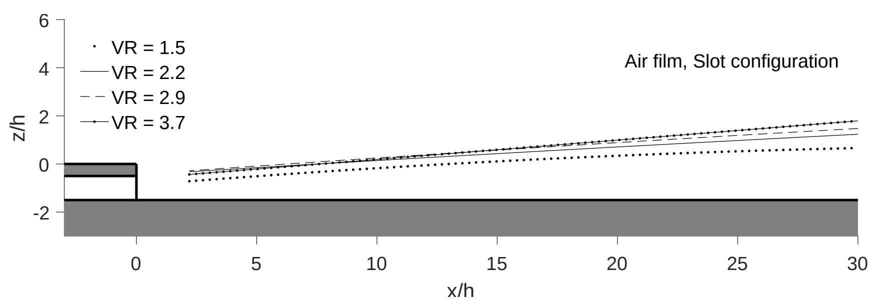

Figure 6: Velocity ratio effects for hole configuration.

Finally, comparison of hole and bar configuration illustrates differences close to the injection point. Figure 7 depicts the position of the boundary layer and velocity profiles of the streamwise velocity component at three locations downstream of the injection step. In this case, CO_2 measurements are chosen, since the differences are easier recognizable. It can be seen that the streamwise velocity close to the hole exit is very low and the boundary layer is located closer to the wall compared to the hole configuration. This shows the effect of the wake region downstream of the bar where three-dimensional structures emerge. About 20 h downstream of the injection step, however, both graphs merge and a homogeneous cooling film is formed.

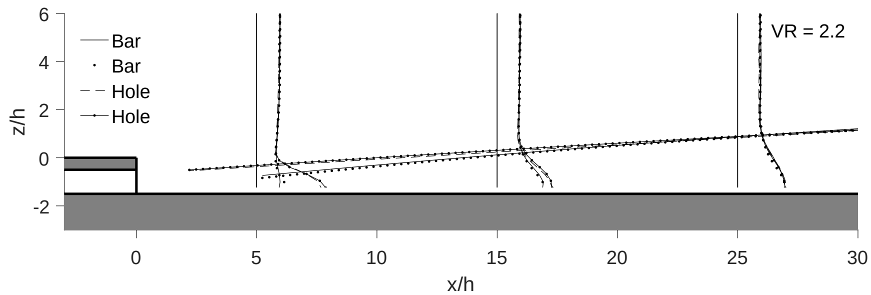

Figure 7: Comparison of hole and bar configuration.

4 Summary and conclusion

Isothermal PIV measurements for planar film injection are carried out. Air and CO_2 are applied as coolants to account for variation of DR. The main flow velocity was set constant while the coolant velocity was varied resulting in different VR. The geometry and flow field are of interest for an future reactive film cooling investigation where PIV measurements are hardly applicable.
The data show that the results for 4 s recording time are acceptable compared to those for 16 s. Considering higher deposition on the glass with increasing time and its negative effect on the post-processing, the short-time experiments are even preferred. Also, the near-wall boundary layer cannot be determined with certainty and is blanked out. The parameter of interest for this study turned out to be the VR. A constant M for air and CO_2 leads to different film thicknesses, whereas a constant VR shows consistent results. Increasing VR thickens the film layer downstream and shows better surface isolation from the main stream. The maximum thickness is around 3.54 mm at a distance of $x/h = 30$. However, the vertical bars in the slot inlet cause a wake region which can be clearly observed by determining the shear and the boundary layer. The surface region after the coolant outlet to some distance might be less protected. Furthermore, the three-dimensional boundary effects may lead to higher coolant-main stream interaction and reach stoichiometric conditions in case of a reactive experiment. The determined shear layer can be compared with the position of secondary combustion in the future reactive study.

References

Evans DS (2008) *The Impact of Heat Release in Turbine Film Cooling*. thesis. Department of the Air Force Air University, Air Force Institute of Technology. Wright-Patterson Air Force Base, Ohio.

Goldstein RJ (1971) Film Cooling. *Advances in Heat Transfer* 7:321–379.

Goldstein RJ and Eckert ERG (1974) Effects of Hole Geometry and Density on Three-Dimensional Film Cooling. *Int J Heat Mass Transfer* 17:595–607.

Johnson B, Tian W, Zhang K, and Hu H (2014) An experimantal study of density ratio effects on the film cooling injection from discrete holes by using PIV and PSP techniques. *International Journal of Heat and Mass Transfer 76, 337-349*

Kostka S, Blunck D, Naibo J, Lynch A, Polanka M, Stouffer S, Gord RR, and Roy S (2011) Temperature of the Inverse Diffusion Flames in a Vitiated Cross-Flow using Two-Color PLIF Thermometry. *Fall Technical Meeting of the Eastern States Section of the Combustion Institute, Storrs, CT*

Richardson DR, Jiang N, Caswell AW, Roy S, Blunck DL, Lynch AC, and Gord JR (2014) Characterization of Inverse Diffusion Flames in High Temperature Cross-flows. *52nd Aerospace Sciences Meeting*

Schreivogel P, Kröss B, and Pfitzner M (2014) Density Ratio Effects on the Flow Field Emanating from Cylindrical Effucion and Trenched Film Cooling Holes. *Preceedings of ASME Turbo Expo 2014, GT2014-25143*

Wieneke B (2015) PIV uncertainty quantification from correlation statisctics. *Meas Sci Technol* 26:074002 (10pp).